Unsteady Aerodynamic Forces for Aeroelastic Analysis of Two-Dimensional Lifting Surfaces

Alexandre N. Marques
ale_noll@yahoo.com
Instituto Tecnológico de Aeronáutica - ITA
12228-900 São José dos Campos, SP. Brazil

Carlos Frederico C. Simões
fred.simoes@pobox.com
EMBRAER - Empresa Brasileira de Aeronáutica
12227-901 São José dos Campos, SP. Brazil

João Luiz F. Azevedo
Member, ABCM
azevedo@iae.cta.br
Instituto de Aeronáutica e Espaço CTA/IAE
12228-903 São José dos Campos, SP. Brazil

The present work is part of an effort for developing a methodology for the aeroelastic analysis of two-dimensional lifting surfaces using an unsteady, Euler-based, CFD tool for the calculation of the aerodynamic operator. The CFD tool solves the flow problem with the finite-volume method applied to an unstructured grid context. The proposed methodology is based on the determination of the aerodynamic operator with the transfer function technique, which is given, in the frequency domain, by the analysis of the system response to an exponentially-shaped pulse in the time domain. The response in the frequency domain is achieved with the Fast Fourier Transform (FFT) technique available in any mathematical manipulation tool, such as Matlab©. Some numerical experiments are performed involving unsteady subsonic and transonic flows around a flat plate and a NACA 0012 airfoil, and the results are presented as curves of generalized aerodynamic forces. The unsteady simulations start from a converged steady state solution obtained by the same CFD tool. Some unsteady validation results are compared with available data in the literature and the initial steps of the methodology are tested. The frequency domain results obtained agree very well with other numerical solutions given in the literature, which validates the present approach for the evaluation of the generalized aerodynamic forces for use in efficient, frequency domain, aeroelastic analyses.
Keywords*: Aeroelasticity, CFD, finite-volume discretization, unsteady aerodynamics, unstructured meshes*

Introduction

Aeroelasticity can be defined as the science which studies the mutual interaction between aerodynamic and structural dynamic forces. The analysis of dynamic characteristics of either complex or simple structures are quite developed nowadays as far as numerical and experimental methods are concerned. Hence, it is correct to state that reliability in aeroelastic calculations, for the problems of interest to the present authors, is strongly dependent on the correct evaluation of the aerodynamic operator.

Traditionally, the methods developed for determining the aerodynamic operator for subsonic and supersonic regimes are based on linearized formulations which do not present the same satisfactory results in the transonic range. According to Tijdeman (1977), this occurs due to the nonlinearity of transonic flows characterizing a significant alteration of the flow behavior, even when a profile is submitted to small perturbations. Ashley (1980) reported the use of semi-empirical corrections to the linearized theory results as a mean of improving flutter predictions. Nevertheless, Ashley (1980) himself believed that really satisfactory aeroelastic quantitative predictions of the transonic regime should be possible only when accurate, three-dimensional, unsteady CFD codes were developed. Hence, the methodology here presented, which is based on the ideas of Rausch, Batina and Yang (1990) and Oliveira (1993), intends to obtain the aerodynamic operator for two-dimensional lifting surfaces employing modern CFD techniques.

Computational Fluid Dynamics (CFD) is a subject that has played an extremely important role in recent studies of aerodynamics. The possibility of treating numerically a broad range of phenomena which occur in flows over bodies of practically any geometry has innumerous advantages over experimental determinations, such as greater flexibility together with time and financial resource savings.

Presented at XI DINAME – International Symposium on Dynamic Problems of Mechanics, February 28th - March 4th, 2005, Ouro Preto. MG. Brazil.
Paper accepted: June, 2005. Technical Editors: J.R.F. Arruda and D.A. Rade.

However, obtaining more reliable numerical results for a growing number of situations has been one of the major recent challenges in many science fields. Fletcher (1988a) and Hirsch (1988) show that particulary in aerodynamics, the general phenomena are governed by the Navier-Stokes equations, which constitute a system of coupled nonlinear partial differential equations that has no general analytical solution and that is of difficult algebraic manipulation. Hirsch (1988) comments, among other issues concerning CFD techniques, on how to simplify the mathematical models conveniently in order to ease the numerical treatment of each case. A survey on this subject is also presented by Azevedo (1990). Space and time discretization schemes, as well as convergence acceleration techniques, boundary condition establishment and other numerical integration tools are available and largely used in order to solve such problems.

After selection of the theoretical model, it is indispensable to define the physical domain where the flow takes place, determining the boundary conditions. This solution approach demands the discrete representation of the physical domain to make the problem numerically coherent by defining a computational mesh of points or regions where the calculations are performed. The mesh generation, as it is vastly documented in the literature, *e.g.* Fletcher (1988b), and verified by the CTA/IAE work group own experience (Bigarella and Azevedo, 2005), is extremely important and decisive in determining the accuracy and convergence of the solution. The mesh type is also an essential factor on the CFD tool behavior. Structured meshes have the advantage of being well-behaved, the existence of an intrinsic correspondence between adjacent nodes and a very good control over grid refinement through stretching functions. However, this sort of mesh do not adapt readily to complicated geometries, requiring the adoption of sophisticated multiblock mesh techniques. On the other hand, unstructured meshes are extremely flexible when it comes to geometric forms and they allow the use of interesting techniques such as adaptative refinement.

As stated by Marques (2004), together with the evolution of the work and projects performed by CTA/IAE, the demand for aerodynamic parameters has increased considerably. In particular, the research group has been charged with the calculation of diverse aerodynamic information concerning the various sounding rockets, satellite launchers and other vehicles developed at CTA/IAE.

Nevertheless, the application of CFD tools in these parametric analyses has always been limited by the need of adequate code development and the lack of computational resources compatible with the work to be performed. Therefore, a progressive approach has been adopted in the development of CFD tools in CTA/IAE and in ITA, as presented by Azevedo (1990), Azevedo, Fico and Ortega (1995), Fico and Azevedo (1994), Azevedo, Strauss and Ferrari (1997), Bigarelli, Mello and Azevedo (1999), Bigarelli and Azevedo (2002), Oliveira (1993), Simões and Azevedo (1999).

The present work is based on the finite-volume formulation, where a CFD tool is applied with unstructured two-dimensional meshes around lifting surfaces to acquire unsteady responses to harmonic and pulse motions. These time-domain responses supply the generalized aerodynamic forces necessary as input to the aeroelastic model. The methodology here presented intends to obtain frequency-domain responses from the solutions to a pulse motion. That information can be used in the future in order to determine the aeroelastic stability margin with a single expensive CFD run per structural mode.

Aerodynamic Theoretical Formulation

The CFD formulation used in this work is based on the two-dimensional Euler equations. Due to the use of unstructured meshes and a finite volume discretization, these equations are used in the Cartesian form. Besides, as usual in CFD applications, flux vectors are employed and the equations are nondimensionalized. Hence, they can be written as

$$\frac{\partial}{\partial t}\iint_V \boldsymbol{Q}\,dxdy + \int_S \left(\boldsymbol{E}dy + \boldsymbol{F}dx\right) = 0. \tag{1}$$

In Eq. (1), V represents the volume of the control volume or, more precisely, its area in the two-dimensional case. S is its surface, or its side edges in 2-D. $\boldsymbol{Q}$ is the vector of conserved properties, given by

$$\boldsymbol{Q} = \left\{\rho \quad \rho u \quad \rho v \quad e\right\}^T. \tag{2}$$

$\boldsymbol{E}$ and $\boldsymbol{F}$ are the flux vectors in the x and y directions, respectively, defined as

$$\boldsymbol{E} = \begin{Bmatrix} \rho U \\ \rho u U + p \\ \rho v U \\ (e+p)U + x_t p \end{Bmatrix}, \tag{3}$$

$$\boldsymbol{F} = \begin{Bmatrix} \rho V \\ \rho u V \\ \rho v V + p \\ (e+p)V + y_t p \end{Bmatrix}. \tag{4}$$

The nomenclature adopted here is the usual in CFD: ρ is the density, u and v are the Cartesian velocity components and e is the total energy per unity of volume. The pressure p is given by the perfect gas equation, written as

$$p = (\gamma - 1)\left[e - \frac{1}{2}\rho\left(u^2 + v^2\right)\right] \tag{5}$$

Once again, as usual, γ represents the ratio of specific heats. The contravariant velocity components (U and V) are determined by

$$U = u - x_t \;\text{ and }\; V = v - y_t, \tag{6}$$

where x_t and y_t are the Cartesian components of the mesh velocity in the unsteady case. For further details on the theoretical formulation, such as boundary and initial conditions, the reader should refer to Marques (2004).

Numerical Formulation

The algorithm here presented is based on a cell-centered finite-volume scheme, in which the stored information is actually the variable average value throughout the entire control volume. These mean values are defined as

$$\boldsymbol{Q}_i = \frac{1}{V_i}\iint_{V_i} \boldsymbol{Q}\,dxdy. \tag{7}$$

Equation (1) can, then, be rewritten for the i-th cell as

$$\frac{\partial}{\partial t}\iint_{V_i} \left(V_i \boldsymbol{Q}_i\right)dxdy + \int_{S_i} \left(\boldsymbol{E}dy - \boldsymbol{F}dx\right) = 0. \tag{8}$$

The remaining integration in Eq. (8) represents the flux of the vector quantities $\boldsymbol{E}$ and $\boldsymbol{F}$ through each control volume's boundary. This code was developed to be used with unstructured meshes composed of triangles. The flux, therefore, can be evaluated as the sum of the flux contributions of each edge, which is obtained approximately from the average with the neighbors' conserved quantities, as proposed by Jameson and Mavriplis (1986). Hence, a convective operator is defined and it is given by

$$\begin{aligned} &\int_{S_i} \left(\boldsymbol{E}dy - \boldsymbol{F}dx\right) \approx C\left(\boldsymbol{Q}_i\right) = \\ &\sum_{k=1}^{3}\left[\boldsymbol{E}\left(\boldsymbol{Q}_{ik}\right)\left(y_{k_2} - y_{k_1}\right) - \boldsymbol{F}\left(\boldsymbol{Q}_{ik}\right)\left(x_{k_2} - x_{k_1}\right)\right], \end{aligned} \tag{9}$$

Where

$$\boldsymbol{Q}_{ik} = \frac{1}{2}\left(\boldsymbol{Q}_i + \boldsymbol{Q}_k\right), \tag{10}$$

and the (x_{k1}, y_{k1}) and (x_{k2}, y_{k2}) coordinates are relative to the vertices which define the interface between the cells.

The Euler equations are a set of nondissipative hyperbolic conservation laws. Hence, as given by Pulliam (1986), their numerical treatment requires an inherently dissipative discretization scheme or the introduction of artificial dissipation terms in order to avoid oscillations near shock waves and to damp high frequency uncoupled error modes. Oliveira (1993) states that the flux evaluation method adopted in the present CFD tool is analogous to a centered difference scheme in finite difference formulation. In this case, Pulliam (1986) shows that there is the necessity of adding artificial dissipation terms. Details on the adopted artificial dissipation scheme are given in Marques (2004).

The numerical solution is advanced in time using a second-order accurate, 5-stage, explicit, hybrid scheme which evolved from the consideration of Runge-Kutta time stepping schemes (Jameson, Schmidt and Turkel, 1981, and Mavriplis, 1990). This scheme, already including the necessary terms to account for changes in cell area due to mesh motion or deformation (Batina, 1989), can be written as

$$
\begin{aligned}
\boldsymbol{Q}_i^{(0)} &= \boldsymbol{Q}_i^{n} \\
\overline{\boldsymbol{Q}}_i &= \frac{V_i^{n}}{V_i^{n+1}} \boldsymbol{Q}_i^{(0)} \\
\Delta \boldsymbol{Q}_i^{(j,k)} &= \frac{\Delta t_i}{V_i^{n+1}} \left[C\left(\boldsymbol{Q}_i^{(j)}\right) - D\left(\boldsymbol{Q}_i^{(k)}\right) \right] \\
\boldsymbol{Q}_i^{(1)} &= \overline{\boldsymbol{Q}}_i - \alpha_1 \Delta \boldsymbol{Q}_i^{(0,0)} \\
\boldsymbol{Q}_i^{(2)} &= \overline{\boldsymbol{Q}}_i - \alpha_2 \Delta \boldsymbol{Q}_i^{(1,1)} \\
\boldsymbol{Q}_i^{(3)} &= \overline{\boldsymbol{Q}}_i - \alpha_3 \Delta \boldsymbol{Q}_i^{(2,1)} \\
\boldsymbol{Q}_i^{(4)} &= \overline{\boldsymbol{Q}}_i - \alpha_4 \Delta \boldsymbol{Q}_i^{(3,1)} \\
\boldsymbol{Q}_i^{(5)} &= \overline{\boldsymbol{Q}}_i - \alpha_5 \Delta \boldsymbol{Q}_i^{(4,1)} \\
\boldsymbol{Q}_i^{n+1} &= \boldsymbol{Q}_i^{(5)},
\end{aligned}
\tag{11}
$$

where the superscripts n and $n+1$ indicate that these are property values at the beginning and the end of the n-th time step, respectively. $D(\boldsymbol{Q})$ denotes the artificial dissipation operator. The values used for the α coefficients, as suggested by Jameson and Mavriplis (1986), are

$$
\alpha_1 = \frac{1}{4},\ \alpha_2 = \frac{1}{6},\ \alpha_3 = \frac{3}{8},\ \alpha_4 = \frac{1}{2},\ \alpha_5 = 1. \tag{12}
$$

In Eq. (11) the convective operator, $C(\boldsymbol{Q})$, is evaluated at every stage of the integration process, but the artificial dissipation operator, $D(\boldsymbol{Q})$, is only evaluated at the two initial stages. This is done with the objective of saving computational time, since the evaluation of the last is rather expensive. As discussed by Jameson, Schmidt and Turkel (1981), this type of procedure is known to provide adequate numerical damping characteristics while achieving the desired reduction in computational cost.

Steady-state solutions for the mean flight condition of interest must be obtained before the unsteady calculation can be started. Therefore, it is also important to guarantee an acceptable efficiency for the code in steady-state mode. In the present work, both local time stepping and implicit residual smoothing (Jameson and Mavriplis, 1986, Jameson and Baker, 1983 and Jameson and Baker, 1987) are employed to accelerate convergence to steady state. More details on convergence acceleration techniques are found in Oliveira (1993) and Marques (2004).

Mesh Generation and Movement

The meshes used in the present work were generated with the commercial grid generator ICEM CFD©, a very powerful tool capable of creating sophisticated meshes with very good refinement and grid quality control. Figures 1(a) and 1(b) show the meshes around a NACA 0012 profile and a flat plate, respectively, which are employed to obtain the results here presented.

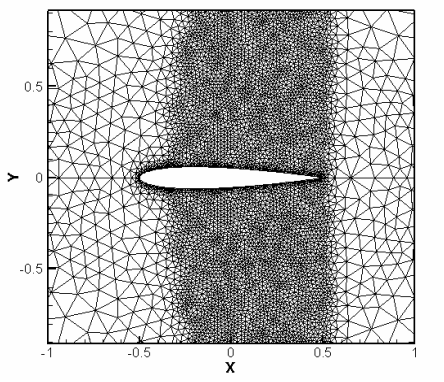

(a)

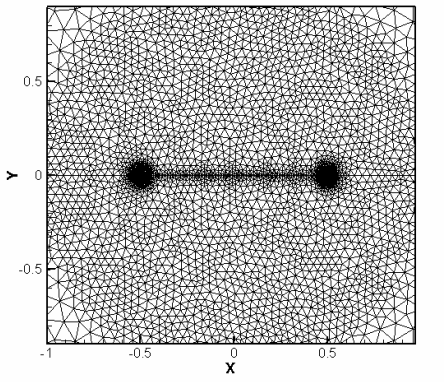

(b)

Figure 1. Mesh around (a) NACA0012 profile with 284 wal points and (b) flat plate with 236 wall points.

Unsteady calculations involve body motion and, therefore, the computational mesh should be somehow adjusted to take this motion into account. The approach adopted here is to keep the far field boundary fixed and to move the interior grid points in order to accommodate the prescribed body motion. This was done following the ideas presented by Batina (1989), and Rausch, Batina and Yang (1990), which model each side of the triangles as a spring with stiffness constant inversely proportional to the length of the side. Hence, once points on the body surface have been moved and assuming that the far field boundary is fixed, a set of static equilibrium equations can be solved for the position of the interior nodes. Control volume areas for the new grid can, then, be computed. For further details, the reader should refer to Marques (2004). The mesh velocity components can also be evaluated considering the new and old point positions and the time step in a geometric conservation law context, as presented by Thomas and Lombard (1979).

Aeroelastic Formulation

The dynamic system represented is the typical section problem (Bisplinghoff, Ashley and Halfman, 1955, and Oliveira, 1993), which is an airfoil section with two degrees of freedom (plunge and pitch) subjected to aerodynamic, dynamic and elastic forces and moments. The governing equation of such dynamic system is given by

$$
[M]\ddot{\boldsymbol{\eta}}(t) + [K]\boldsymbol{\eta}(t) = \boldsymbol{Q_a}(t), \tag{13}
$$

where the generalized mass and stiffness matrices are, respectively, given by

$$[M]=\begin{bmatrix} 1 & x_\alpha \\ x_\alpha & r_\alpha^2 \end{bmatrix}, \tag{14}$$

$$[K]=\begin{bmatrix} \omega_h^2 & 0 \\ 0 & r_\alpha^2\omega_\alpha^2 \end{bmatrix}, \tag{15}$$

and the generalized coordinate and force vectors are, respectively,

$$\boldsymbol{\eta}(t)=\{\xi(t) \quad \alpha(t)\}^T, \tag{16}$$

$$\boldsymbol{Q_a}(t)=\left\{\frac{Q_h(t)}{mb} \quad \frac{Q\alpha(t)}{mb^2}\right\}^T. \tag{17}$$

In the previous equations, ω_h and ω_α are the uncoupled free vibration circular frequencies of each mode, which are defined as

$$\omega_h=\left(\frac{k_h}{m}\right)^{1/2}, \qquad \omega_\alpha=\left(\frac{k_\alpha}{I_\alpha}\right)^{1/2}, \tag{18}$$

where k_h and k_α are the stiffness constants in the plunge and pitch modes. Besides, m denotes the section mass and I_α its inertia moment respective to the elastic axis over which pitch takes place. Moreover, $\xi = h/b$, where h is the plunge amplitude and b the airfoil semi-chord. Finally, the radius of gyration is given by

$$r_\alpha=\left(\frac{I_\alpha}{mb^2}\right)^{1/2}. \tag{19}$$

This system can be more easily studied in the Laplace domain. Applying the Laplace transform on Eq. (13), one can obtain

$$s^2[M]\boldsymbol{\eta}(s)+[K]\boldsymbol{\eta}(s)=\boldsymbol{Q_a}(s). \tag{20}$$

Therefore, as mentioned before, the main objective of the present study is to efficiently determine the generalized aerodynamic force vector ***Qa****(s)* in the Laplace domain for the transonic regime. This is done by evaluating this vector over the frequency range of interest and, through analytical continuation (see Churchill, Brown and Verhey, 1974) extend such result to the entire *s*-plane.

Aeroelastic Analysis Methodology

The unsteady movements related to the aeroelastic phenomena, mainly flutter, can be represented by a series of harmonic motions. Therefore, a large computational cost reduction comes from the use of the indicial method. According to this approach, the aerodynamic response to a harmonic excitation of any frequency can be obtained from Duhamel's integral of the response of the flow to an indicial motion. Following this same idea, and noticing that the transient flow due to an impulsive excitation takes a shorter period of time to die out than those that results from an indicial motion, Oliveira (1993) proposed a similar methodology where the aerodynamic response is evaluated in the frequency domain from the response to a impulsive excitation in the time domain.

Therefore, the aerodynamic calculations for a determined flight condition are reduced to a single computational run for each structural mode. Such an approach can lead to a drastic reduction in the computational cost of aeroelastic analyses using a nonlinear aerodynamic formulation. To be more precise, the present approach considers that the generalized aerodynamic forces can be constructed by the superposition of the effects of each modal displacement evaluated separately. Clearly, this means that the formulation is correct for small displacement amplitudes. However, since classical airfoil or wing flutter are the main concern in the present case, this does not constitute any major limitation because flutter onset is the condition sought. Hence, the present approach guarantees that the flow nonlinearities and dynamics are captured, except for those related to viscous effects which are not included in an Euler formulation.

Nevertheless, the theoretical impulse is a singularity and the indicial motion leads to the appearance of infinite velocities, which makes both numerically untreatable. Hence, other smoother excitation functions are employed (Davies and Salmond, 1980, and Mohr, Batina and Yang, 1989). The motion suggested by Bakhle et al. (1991) is defined as

$$fp(t)=\begin{cases} 4\left(\dfrac{\bar{t}}{\bar{t}_{\max}}\right)^2 e^{\left(2-\frac{1}{1-\frac{\bar{t}}{\bar{t}_{\max}}}\right)}; & 0\le\bar{t}\le\bar{t}_{\max}, \\ 0; & \bar{t}\ge\bar{t}_{\max}, \end{cases} \tag{21}$$

where the bar indicates the dimensionless time and $\bar{t}_{\max}$ is the exponentially-shaped pulse duration. As can be seen in Fig. 2, the function defined in Eq. (21) guarantees a smooth motion.

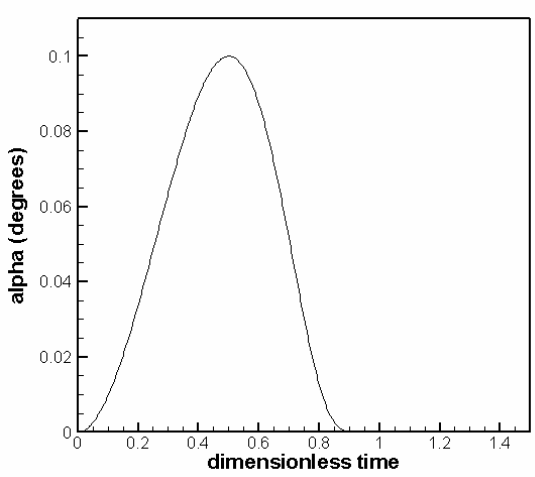

Figure 2. Exponentially-shaped pulse excitation in angle of attack.

The methodology consists, then, in obtaining a transfer function in the frequency domain applicable to any desirable input. This transfer function is the frequency domain response to the impulsive excitation. Therefore, this is accomplished using the following steps:

- Obtaining the steady aerodynamic solution for a given Mach number and angle of attack;
- Performing unsteady aerodynamic response evaluations departing from the steady solution given in the previous item. This stage leads to time responses in terms of aerodynamic coefficients as a result to an exponentially-shaped pulse excitation of each of the modes;
- Obtaining the Fourier transform of the time responses applying a Fast Fourier Transform (FFT) algorithm. This is done in the present work employing the FFT capability available in the commercial program Matlab©;

• Approximating the obtained data with an interpolating polynomial, shown in Oliveira (1993);

• Formulating the corresponding eigenvalue problem, valid for a determined range of dimensionless velocities, and, finally, flutter speed prediction through a root locus analysis.

As shown by Oliveira (1993), the corresponding frequency domain resulting from the FFT procedure is given by

$$\begin{aligned} f &= \frac{1}{\Delta t}\frac{i}{N} \\ &= \frac{a_\infty}{\Delta \bar{t} c}\frac{i}{N}; \quad i = 0,1,2,...,N_{\max}, \end{aligned} \tag{22}$$

$$N_{\max} = \begin{cases} N/2; \\ (N-1)/2; \end{cases} \text{ if } N \text{ even, otherwise,} \tag{23}$$

where c is the chord length and a_∞ the freestream speed of sound. Equation (22), rewritten in terms of the reduced frequency based on the semi-chord (b), stands as

$$\begin{aligned} k &= \frac{\omega b}{U_\infty} = \frac{2\pi f b}{U_\infty}, \\ &= \frac{\pi}{M_\infty \Delta \bar{t}}\frac{i}{N}; \quad i = 0,1,2,...,N_{\max} \end{aligned} \tag{24}$$

where M_∞ is the Mach number referring to the undisturbed conditions.

As the input is not exactly an impulse excitation, the real impulse response is evaluated using the convolution integral concept and its well-known property, as given by Brigham (1988)

$$g(t) = fp(t) * i(t) \Rightarrow G(f) = Fp(f) I(f), \tag{25}$$

$$I(f) = \frac{G(f)}{Fp(f)}. \tag{26}$$

where $i(t)$ represents the time response to a impulsive movement and $g(t)$ is the response to the smooth excitation given in Eq. (21). The functions in capital letters are discrete Fourier transforms of the corresponding functions in low case letters. Therefore, after obtaining the FFT of the time response, it has to be divided by the FFT of the input pulse function. Although the input is not the exact impulsive excitation, it is capable of exciting the reduced frequencies of interest in aeroelastic studies.

Results and Discussion

Before attempting applications of the proposed methodology, some validation simulations were performed with the CFD tool. This has been done throughout the entire development of this code as can be seen in Azevedo (1992), Oliveira (1993) and Simões and Azevedo (1999). The present authors proceeded with this effort obtaining the results shown in Figs. 3 to 7 for a NACA 0012 airfoil at M_∞ = 0.755 submitted to a harmonic pitching motion about the quarter-chord point. The motion's reduced frequency is k = 0.0814 and the amplitude is 2.51º, while the mean angle of attack is 0.016º. Figures 3, 4 and 5 present the pressure coefficient along the chord in different positions of the cycle and compares them with results presented by Batina (1989), which are also obtained numerically with a CFD tool similar to the one employed in the present work. The solutions in terms of aerodynamic coefficient hysteresis curves are given in Figs. 6 and 7, together with experimental data from AGARD (1982). The value of C_m is referred to the quarter-chord point. The present results are very close to those obtained by Batina (1989). Some small differences appear near shocks and the authors believe that they are due to the use of a more refined mesh in the present work. Moreover, the deviations between numerical and experimental results seem to be systematic and caused by experimental data reduction errors.

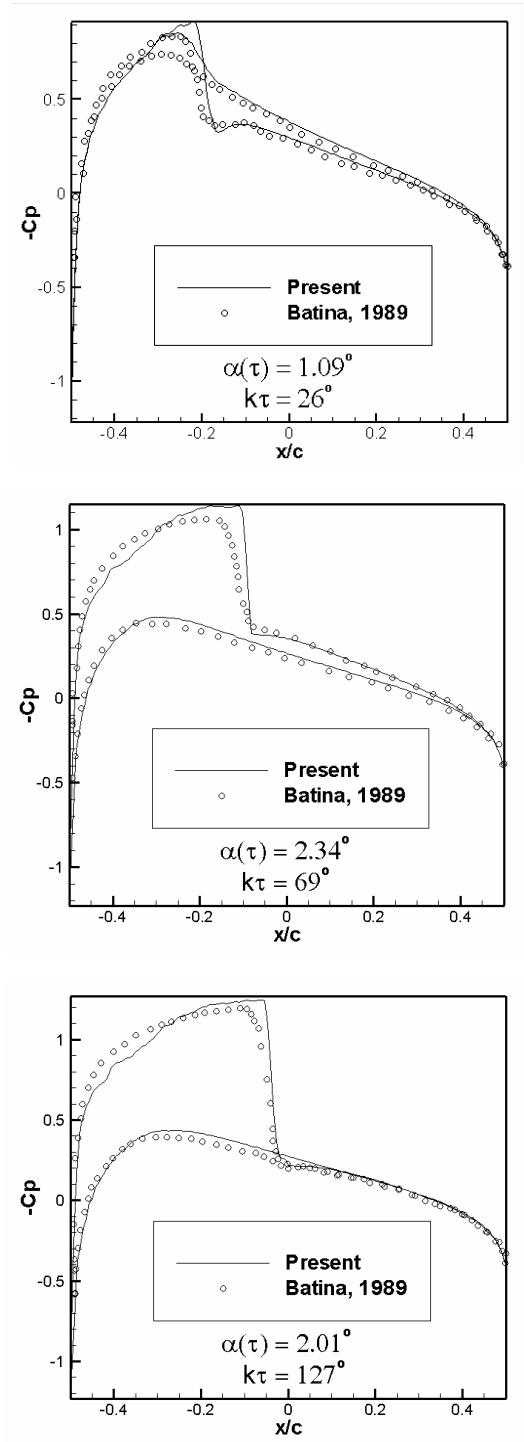

Figure 3. Comparison of instantaneous pressure distributions for the NACA 0012 airfoil in pitching motion – Part I.

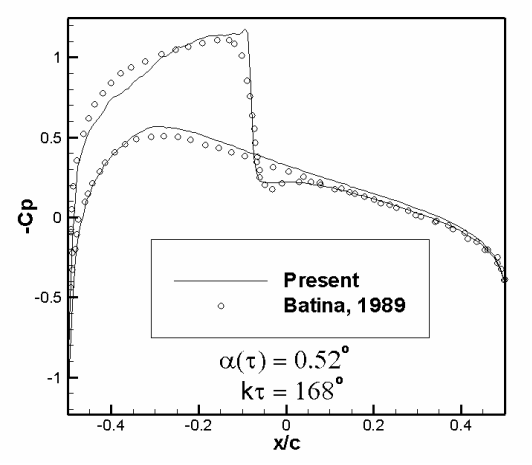

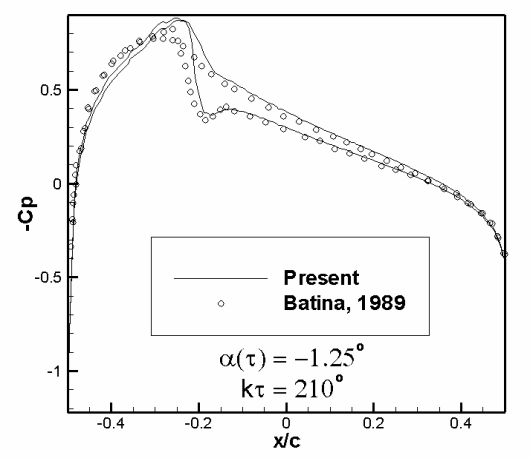

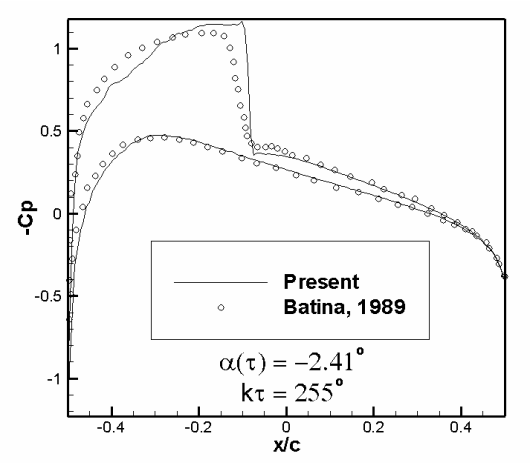

Figure 4. Comparison of instantaneous pressure distributions for the NACA 0012 airfoil in pitching motion – Part II.

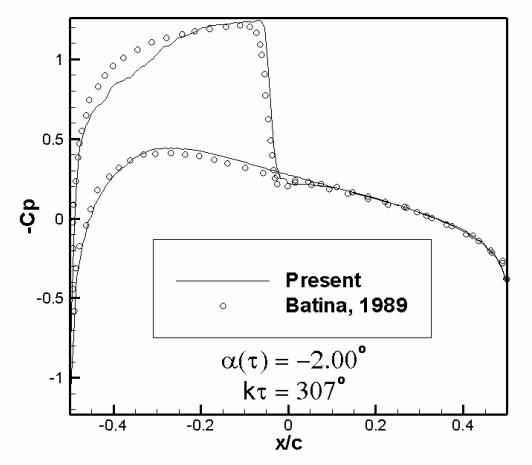

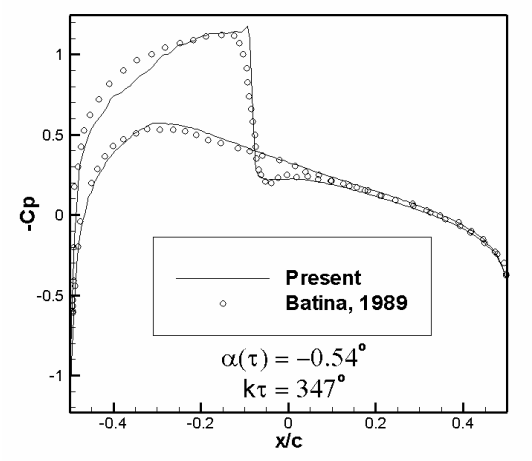

Figure 5. Comparison of instantaneous pressure distributions for the NACA 0012 airfoil in pitching motion – Part III.

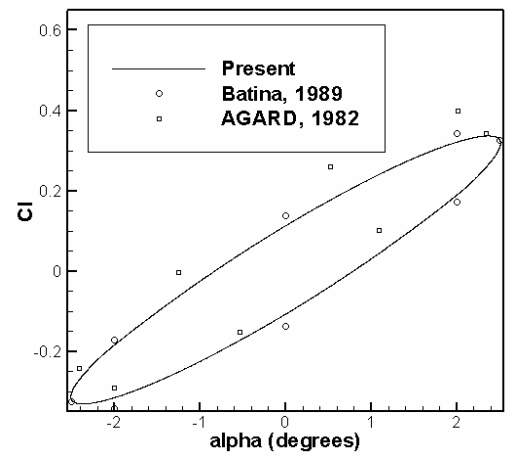

Figure 6. Cl hysteresis curve.

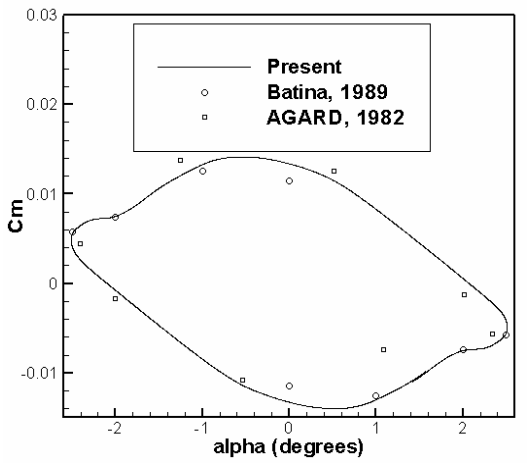

Figure 7. Cm hysteresis curve.

Once the CFD tool was tested and proved to be a reliable one, the next step was to proceed in obtaining the responses of interest for the aeroelastic analysis methodology proposed. The approach selected was to reproduce the results presented by Rausch, Batina and Yang (1990). This reference presents the aerodynamic coefficient response in the frequency domain obtained with a pulse transfer function approach, very similar to the methodology proposed here. Therefore, initially, the response of a flat plate airfoil to an exponentially-shaped excitation at $M_\infty = 0.5$ is presented. This response was obtained for pitching motion about the quarter-chord point, Figs. 8 and 9, and for plunging motion, Figs. 10 and 11. Note that no time response to this particular excitation is available in the literature. Hence, the results cannot be compared.

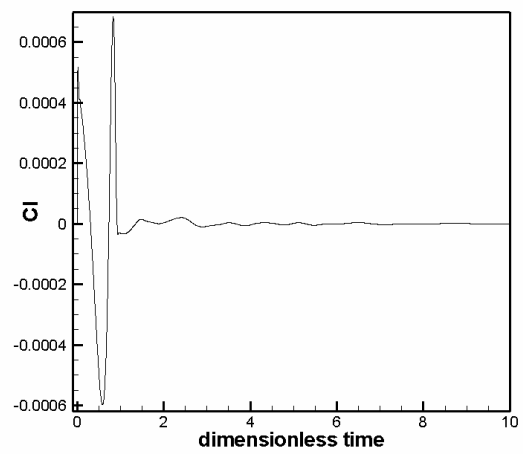

Figure 8. Cl response along time to an exponentially-shaped pulse excitation in pitch mode. Flat plate at M_∞ = 0.5.

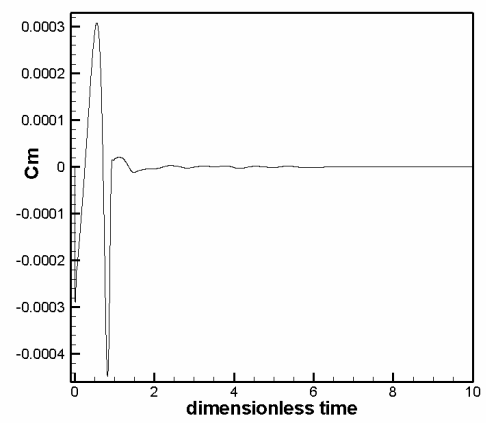

Figure 9. Cm response along time to an exponentially-shaped pulse excitation in pitch mode. Flat plate at M_∞ = 0.5.

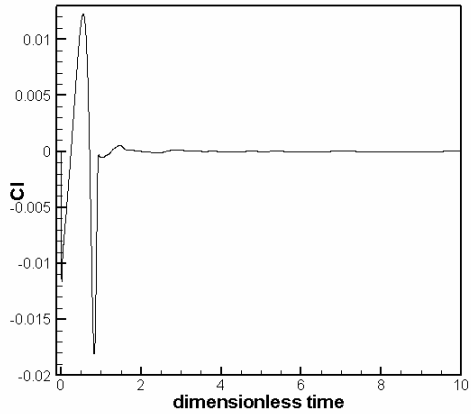

Figure 10. Cl response along time to an exponentially-shaped pulse excitation in plunge mode. Flat plate at M_∞ = 0.5.

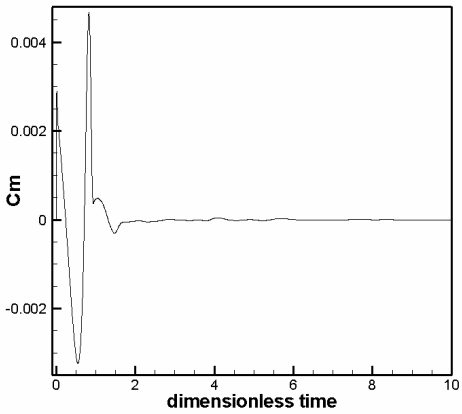

Figure 11. Cm response along time to an exponentially-shaped pulse excitation in plunge mode. Flat plate at M_∞ = 0.5.

The corresponding Fourier transform, together with the results given by Rausch, Batina and Yang (1990), are shown in Figs. 12 to 15. These results indicate a very good agreement between calculations performed with the proposed method and the literature data.

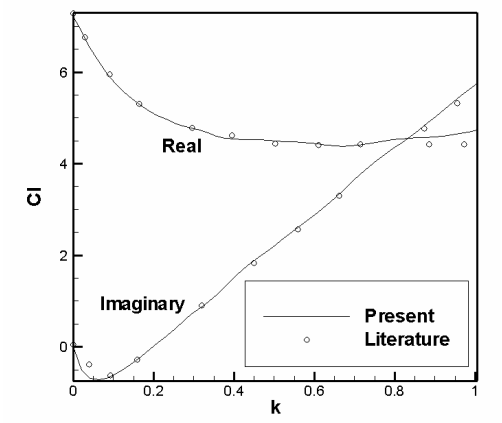

Figure 12. Cl response in frequency domain to an exponentially-shaped pulse excitation in pitch mode. Flat plate at M_∞ = 0.5.

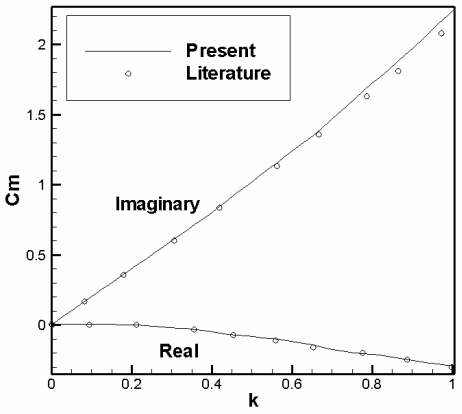

Figure 13. Cm response in frequency domain to an exponentially-shaped pulse excitation in pitch mode. Flat plate at M_∞ = 0.5.

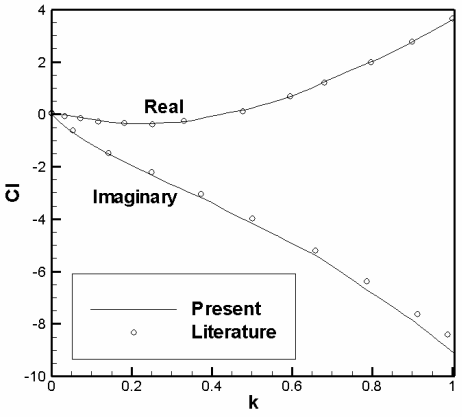

Figure 14. Cl response in frequency domain to an exponentially-shaped pulse excitation in plunge mode. Flat plate at M_∞ = 0.5.

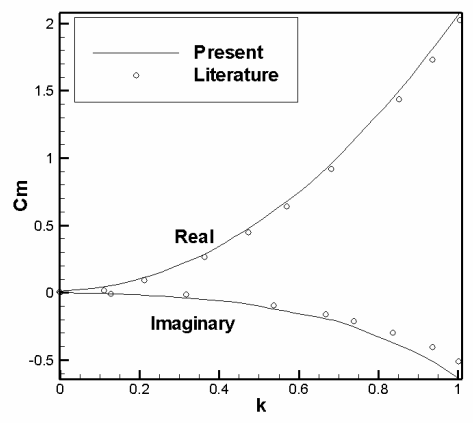

Figure 15. Cm response in frequency domain to an exponentially-shaped pulse excitation in plunge mode. Flat plate at M_∞ = 0.5.

However, the previously discussed results are purely subsonic and this is not the real subject of interest of the present study. Therefore, the authors considered the same sort of analysis for a NACA 0012 airfoil at M_∞ = 0.8, for which case results are also found in Rausch, Batina and Yang (1990). The time response for this test case in terms of C_l and C_m are presented for pitching about the quarter-chord and plunging in Figs. 16 to 19.

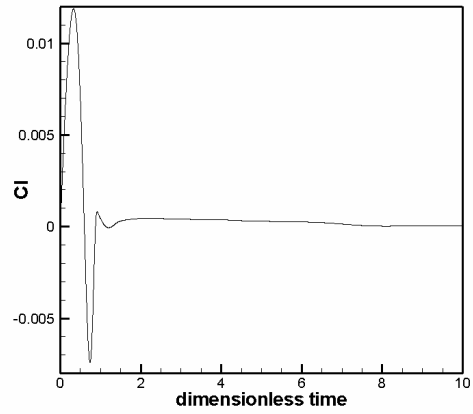

Figure 16. Cl response along time to an exponentially-shaped pulse excitation in pitch mode. NACA 0012 airfoil at M_∞ = 0.8.

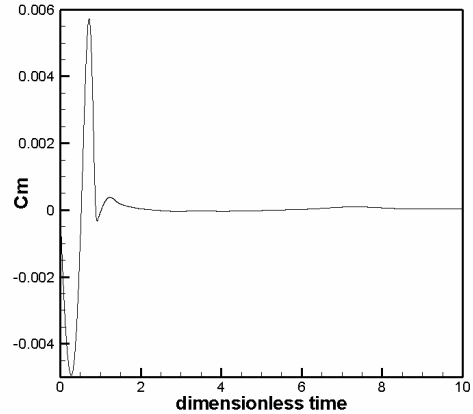

Figure 17. Cm response along time to an exponentially-shaped pulse excitation in pitch mode. NACA 0012 airfoil at M_∞ = 0.8.

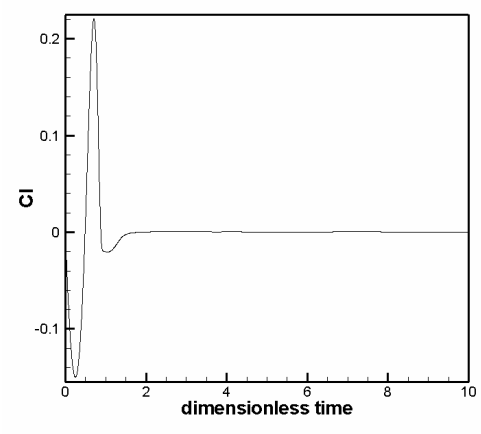

Figure 18. Cl response along time to an exponentially-shaped pulse excitation in plunge mode. NACA 0012 airfoil at M_∞ = 0.8.

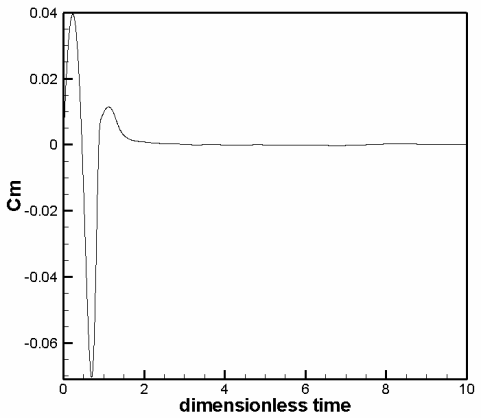

Figure 19. Cm response along time to an exponentially-shaped pulse excitation in plunge mode. NACA 0012 airfoil at M_∞ = 0.8.

The Fourier transforms of such aerodynamic coefficient time histories are shown in Figs. 20 to 23 together with the results presented by Rausch, Batina and Yang (1990). Once again, the results obtained in the present work agree very well with those given in the literature. Therefore, the present test case indicates that the first three items of the proposed methodology for aeroelastic analysis have already been successfully implemented. The work performed comprises the evaluation of the aerodynamic forces using CFD methods. Hence, the current results demonstrate that the unsteady aerodynamic forces are being correctly evaluated and the approach is able to yield the required coefficients, in the frequency domain, for the desired aeroelastic stability analyses.

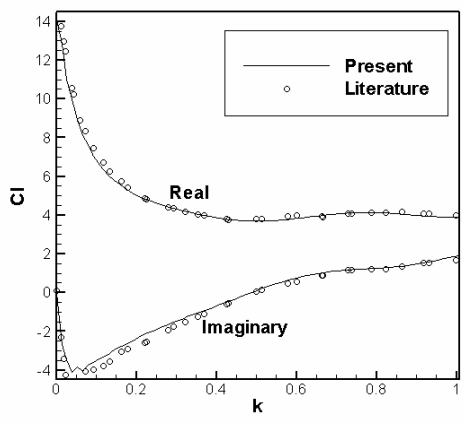

Figure 20. Cl response in frequency domain to an exponentially-shaped pulse excitation in pitch mode. NACA 0012 airfoil at M_∞ = 0.8.

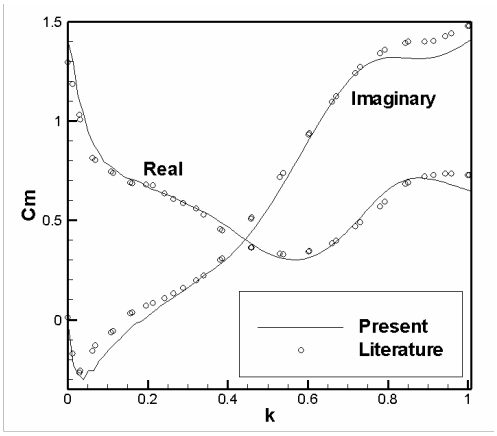

Figure 21. Cm response in frequency domain to an exponentially-shaped pulse excitation in pitch mode. NACA 0012 airfoil at M_∞ = 0.8.

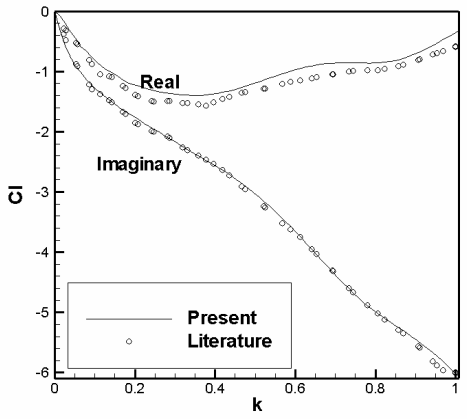

Figure 22. Cl response in frequency domain to an exponentially-shaped pulse excitation in plunge mode. NACA 0012 airfoil at M_∞ = 0.8.

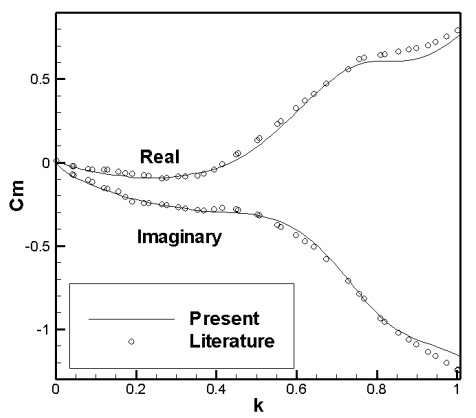

Figure 23. Cm response in frequency domain to an exponentially-shaped pulse excitation in plunge mode. NACA 0012 airfoil at M_∞ = 0.8.

Concluding Remarks

This work comprises the evaluation of all the required aerodynamic data in the frequency domain for use together with the proposed aeroelastic analysis methodology. Therefore, the frequency domain results obtained through the execution of the steps demonstrated in the present work completely represent the aerodynamic behavior involved in the aeroelastic phenomena of interest.

As one can see in the results presented and other cited references, the CFD tool developed by the CTA/IAE group has been widely tested and it has proved to be a reliable source of unsteady aerodynamic data for aeroelastic use in the subsonic and transonic regimes. Furthermore, the frequency domain data obtained in the present work agree very well with other numerical experiments available in the literature, which indicates the correct implementation of the aerodynamic operator for the proposed methodology.

Therefore, such excellent results encourage the authors to move forward to achieve the complete implementation of the aeroelastic analysis methodology proposed. The implementation and validation of the remaining steps of this methodology, which are beyond the scope of the present work, will provide the required capabilities to study aeroelastic problems using an efficient approach in the frequency domain. Therefore, in this context, the present work represents a fundamental research development to the evolution of computational aeroelastic studies for the aerospace configurations of interest to CTA/IAE.

Acknowledgments

The authors gratefully acknowledge the partial support for this research provided by Conselho Nacional de Desenvolvimento Científico e Tecnológico, CNPq, under the Integrated Project Research Grant N°. 501200/2003-7. The first author was also supported by a FAPESP MS scholarship under Grant N°. 04/11200-1.

References

AGARD Report No. 702, 1982, "Compendium of Unsteady Aerodynamic Measurements".

Ashley, H., 1980, "Role of Shocks in the "Sub-Transonic" Flutter Phenomenon," *Journal of Aircraft*, Vol. 17, No. 3, pp. 187-197.

Azevedo, J.L.F., 1990, "Euler Solutions of Transonic Nozzle Flows," Proceedings of the 3rd National Meeting on Thermal Sciences - III ENCIT, Itapema, SC, Brazil, pp. 243-248.

Azevedo, J.L.F., 1992, "On the Development of Unstructured Grid Finite Volume Solvers for High Speed Flows," Report NT-075-ASE-N/92, Instituto de Aeronáutica e Espaço, São José dos Campos, SP (also available as Report No. 91/9, Institut für Strömungsmechanik, T.U. Braunschweig, F.R. Germany, Dec. 1992).

Azevedo, J.L.F., Fico, N.G.C.R., Jr. and Ortega, M.A., 1995, "Two-Dimensional and Axisymmetric Nozzle Flow Computation Using the Euler Equations," *Journal of the Brazilian Society of Mechanical Sciences and Engineering*, Vol. 17, No. 2, pp. 147-170.

Azevedo, J.L.F., Strauss, D. and Ferrari, M.A.S., 1997, "Viscous Multiblock Simulations of Axisymmetric Launch Vehicle Flows," AIAA Paper No. 97-2300, 15th AIAA Applied Aerodynamics Conference, Atlanta, GA.

Bakhle, M.A., Mahjan, A.J., Keith, T.G., Jr. and Stefko, G.L., 1991, "Cascade Flutter Analysis with Transient Response Aerodynamics," *Computers and Structures*, Vol. 41, No. 5, pp. 1073-1085.

Batina, J.T., 1989, "Unsteady Euler Airfoil Solutions Using Unstructured Dynamic Meshes," AIAA Paper 89-0115, 27th Aerospace Sciences Meeting, Reno, NV.

Bigarella, E.D.V. and Azevedo, J.L.F., 2005, "A Study of Convective Flux Computation Schemes for Aerodynamic Flows," AIAA Paper No. 2005-0633, 43rd AIAA Aerospace Sciences Meeting and Exhibit, Reno, NV.

Bigarelli, E.D.V., Mello, O.A.F. and Azevedo, J.L.F., 1999, "Three Dimensional Flow Simulations for Typical Launch Vehicles at Angle of Attack," Proceedings of the 15th Brazilian Congress on Mechanical Engineering - COBEM 1999, Águas de Lindóia, SP.

Bigarelli, E.D.V. and Azevedo, J.L.F., 2002, "On Turbulence Models for 3-D Aerospace Applications," Proceedings of the 9th Brazilian Congress of Thermal Engineering and Sciences, Paper CIT02-0341, Caxambu, MG.

Bisplinghoff, H.L., Ashley, H. and Halfman, R.L., 1955, *Aeroelasticity*, Addison-Wesley, Cambridge, MA.

Brigham, E.O., 1988, *The Fast Fourier Transform and its Applications*, Prentice Hall, Englewood Cliffs, New Jersey.

Churchill R.V., Brown J.W., and Verhey, R.F., 1974, *Complex Variables and Applications*, 3rd ed., McGraw-Hill, New York, NY.

Davies, D. and Salmond, D.J., 1980, "Indicial Approach to Harmonic Perturbations in Transonic Flow," *AIAA Journal*, Vol. 18, No. 8, pp. 1012-1014.

Fico, N.G.C.R., Jr. and Azevedo, J.L.F., 1994, "Numerical Investigation of Supersonic Flow in a Slotted Wind Tunnel," Proceedings of the 15th Iberian Latin-American Congress on Computational Methods for Engineering - XV CILAMCE, Belo Horizonte, MG, pp. 314-322.

Fletcher, C.A.J., 1988a, *Computational Techniques for Fluid Dynamics - Fundamental and General Techniques*, Vol. I, Springer Verlag, Berlin.

Fletcher, C.A.J., 1988b, *Computational Techniques for Fluid Dynamics - Specific Techniques for Different Flow Categories*, Vol. II, Springer Verlag, Berlin.

Hirsch, C., 1988, *Numerical Computation of Internal and External Flows - Fundamental of Numerical Discretization*, Vol. I, John Wiley & Sons, Chichester, NY.

Jameson, A. and Mavriplis, D., 1986, "Finite Volume Solution of the Two-Dimensional Euler Equations on a Regular Triangular Mesh," *AIAA Journal*, Vol. 24, No. 4, pp. 611-618.

Jameson, A. and Baker, T.J., 1983, "Solution of the Euler Equation for Complex Configurations," AIAA Paper 83-1929.

Jameson, A. and Baker, T.J., 1987, "Improvements to the Aircraft Euler Method," AIAA Paper 87-0452, AIAA 25th Aerospace Sciences Meeting, Reno, NV.

Jameson, A., Schmidt, W. and Turkel, E., 1981, "Numerical Solution of the Euler equations by Finite Volume Methods Using Runge-Kutta Time-Stepping Schemes," AIAA Paper 81-1259, AIAA 14th Fluid and Plasma Dynamics Conference, Palo Alto, CA.

Marques, A.N., 2004, Simulation of Unsteady Aerospace Flows Using Unstructured Meshes, Graduation Project, Instituto Tecnológico de Aeronáutica, São José dos Campos, SP, Brazil (in Portuguese, original title is "Simulação de Escoamentos Aeroespaciais não Estacionários Utilizando Malhas não Estruturadas").

Mavriplis, D.J., 1990, "Accurate Multigrid Solution of the Euler Equations on Unstructured and Adaptative Meshes," *AIAA Journal*, Vol. 28, No. 2, pp. 213-221.

Mohr, R.W., Batina, J.T. and Yang, H.T.Y., 1989, "Mach Number Effects on Transonic Aeroelastic Forces and Flutter Characteristics," *Journal of Aircraft*, Vol. 26, No. 11, pp. 1038-1046.

Oliveira, L.C., 1993, "A State-Space Aeroelastic Analysis Methodology Using Computational Aerodynamics Techniques," Master Thesis, Instituto Tecnológico de Aeronáutica, São José dos Campos, SP, Brazil (in

Portuguese, original title is “Uma Metodologia de Análise Aeroelástica com Variáveis de Estado Utilizando Técnicas de Aerodinâmica Computacional”).

Pulliam, T.H., 1986, “Artificial Dissipation Models for the Euler Equations,” *AIAA Journal*, Vol. 24, No. 12, pp. 1931-1940.

Rausch, R.D., Batina, J.T. and Yang, H.T., 1990, “Euler Flutter Analysis of Airfoil Using Unstructured Dynamic Meshes,” *Journal of Aircraft*, Vol. 27, No. 5, pp. 436-443.

Simões, C.F.C. and Azevedo, J.L.F., 1999, “The Influence of Numerical Parameters on Unsteady Airfoil Inviscid Flow Simulations Using Unstructured Dynamic Meshes,” Proceedings of the 15th Brazilian Congress on Mechanical Engineering - COBEM 1999, Águas de Lindóia, SP.

Thomas, P.D. and Lombard, C.K., 1979, “Geometric Conservation Law and Its Application to Flow Computations on Moving Grids,” *AIAA Journal*, Vol. 17, No. 10, pp. 1030-1037.

Tijdeman, H., 1977, “Investigation of the Transonic Flow Around Oscillating Airfoils,” NLR-TR-77090U, National Aerospace Laboratory, The Netherlands.